European Journal of Pharmaceutical Sciences 106 (2017) 287–293

Contents lists available at ScienceDirect

European Journal of Pharmaceutical Sciences

journal homepage: www.elsevier.com/locate/ejps

siRNA delivery system based on magnetic nanovectors: Characterization and stability evaluation

Mohammed Abdelrahman[a,b], Laurence Douziech Eyrolles[a,*], Suad Y. Alkarib[c], Katel Hervé-Aubert[a], Sanaa Ben Djemaa[a], Hervé Marchais[a], Igor Chourpa[a], Stephanie David[a]

[a] Université François-Rabelais de Tours, EA 6295 Nanomédicaments et Nanosondes, 31 Avenue Monge, 37200 Tours, France
[b] Department of Pharmaceutics, Faculty of Pharmacy, University of Gezira, P.O. Box 20, Wad Medani, Sudan
[c] Department of Pharmaceutics, College of Pharmacy, Karary University, Khartoum, Sudan

ARTICLE INFO

Keywords:
Small interfering RNA
Magnetic siRNA nanovectors (MSN)
Superparamagnetic iron oxide nanoparticles (SPION)
Capillary electrophoresis (CE)
Purification

ABSTRACT

Gene therapy and particularly small interfering RNA (siRNA) is a promising therapeutic method for treatment of various human diseases, especially cancer. However the lack of an ideal delivery system limits its clinical applications. Effective anticancer drug development represents the key for translation of research advances into medicines. Previously we reported, the optimization of magnetic siRNA nanovectors (MSN) formulation based on superparamagnetic iron oxide nanoparticles (SPION) and chitosan for systemic administration.

This work aimed at using rational design to further optimize and develop MSN. Therefore, formulated MSN were first purified, then their physical and chemical properties were studied mainly through capillary electrophoresis. 95% of siRNA was found enclosed within the purified MSN (pMSN). pMSN showed colloidal stability at pH 7.4, effective protection of siRNA against ribonuclease degradation up to 24 hours and few siRNA release (less than 10%) at pH 7.4. These findings push toward further evaluation studies *in vitro* and/or *in vivo*, indicating the appropriateness of pMSN for cancer theranostics.

1. Introduction

Current challenges to develop innovative and effective systemic delivery systems aiming to improve gene therapy include a significant time and cost involvement with very low success rates. These have led to increasing efforts toward enhancing the effectiveness of the development process and to minimize failure of candidates at later stages of development to achieve the translation of research advances into medicines. These efforts include particularly the rational design of new formulations, *i.e.* the strategy of creating a new delivery system by adding components with known properties and the characterization and stability evaluation of this delivery system in different conditions permitting to predict how the delivery system's structure will affect its behavior after administration *in vivo*. Thus, to predict the behavior of the delivery system, it is essential to well characterize the delivery system and to evaluate its stability. Therefore, increasing emphasis has been placed on developing a mechanistic understanding of the physicochemical and biological phenomena involved in gene therapy delivery system development such as chemical, physical and biological stability (Haussecker, 2014).

Gene therapy and particularly small interfering RNA (siRNA) is a promising tool for treatment of various diseases, especially cancer. siRNA can cause specific down regulation of proteins through RNA interference (RNAi) inducing either degradation of mRNA or inhibition of the translation (Buschmann et al., 2013; Meister and Tuschl, 2004). In theory, siRNA has great advantages, such as high degree of safety, high efficacy, unrestricted choice of targets and specificity (Xu and Wang, 2015). However, siRNA applications are limited by its intrinsic properties such as short plasma half-life, lack of specific biodistribution and poor membrane permeability. In consideration of these limitations, and for realizing the broad potential of siRNA-based therapeutics, suitable, safe and effective siRNA delivery methods are desired.

Nonviral Nanometer-scaled Drug Delivery Systems (Nano DDSs) represent a flexible and growing technology that is expected to become of high importance in cancer therapy and diagnosis (theranosis) in the near future. Regarding cancer theranosis, Bennett et al. classified Nano DDSs according to the component carrier materials into metal particles, polymeric particles, vesicles, nanomicelles, *etc.*… (Bennett et al., 2014). Among them, siRNA nanocarriers based on functionalized Superparamagnetic Iron Oxide Nanoparticles (SPION) have attracted increasing attention because of their magnetic properties, low cost and easy synthesis and well-defined functionalization protocols (Devarasu

* Corresponding author at: EA 6295 Nanomédicaments et Nanosondes, 31 Avenue Monge, Université François-Rabelais de Tours, 37200 Tours, France.
E-mail address: douziech.eyrolles@univ-tours.fr (L. Douziech Eyrolles).

http://dx.doi.org/10.1016/j.ejps.2017.05.062
Received 31 January 2017; Received in revised form 18 May 2017; Accepted 29 May 2017
Available online 01 June 2017
0928-0987/

et al., 2013). SPION are highly magnetized in magnetic field, allowing magnetic tumor targeting and biomedical magnetic resonance imaging (MRI) (Estelrich et al., 2015).

For treatment of most cancers, systemic routes of siRNA delivery are needed. The design criteria of an *in vivo* systemic siRNA delivery system should include biocompatibility, biodegradability, and non-immunogenicity. Additionally, the system should protect siRNA from serum nucleases and deliver it into target cells efficiently. Finally, the delivery system should provide siRNA an endosome escape ability to enter the RNAi machinery and activate RNAi pathways (Juliano et al., 2008). To solve the delivery problems of siRNA, many delivery systems have been developed. These delivery systems are quite different in terms of structure, size and chemistry, but there are still some deficiencies regarding the characteristics of optimal delivery systems.

Magnetic siRNA nanovectors (MSN) composed of silanised SPION, chitosan and siRNA were recently developed in our laboratory (David et al., 2013). MSN were formulated *via* electrostatic deposition of siRNA and chitosan layers on the surface of the magnetic core made of aminosilane-coated SPION (SPION-NH_3^+). The formulation parameters used were those determined in our previous study to obtain MSN with a hydrodynamic diameter (D_H, *i.e.* the apparent size of hypothetical spherical hydrated/solvated MSN) around 100 nm, suitable for systemic administration (David et al., 2014). For some experiments, in order to improve the sensitivity of analytical methods, we replaced native siRNA by siRNA labeled with a fluorochrome Alexa 488, hereafter called Fl.siRNA.

The present paper aimed at optimizing systemic siRNA magnetic nanovector using rational formulation design. Therefore, formulated MSN were purified and their physical, chemical and biological stability was determined. Many nanoparticles purification methods are described in the literature such as dialysis, ultrafiltration, ultracentrifugation and size exclusion chromatography (SEC). Among these methods, we have used centrifugation which represents a good compromise between easiness and efficiency (Limayem et al., 2004; Pedro et al., 2008).

The detailed MSN characterization has been achieved using a spectrum of biochemical and analytical techniques, including capillary electrophoresis (CE), agarose gel electrophoresis (AGE) and UV–visible spectrophotometry. Due to its specificity, short detection time and small volume of samples used (Li et al., 2014), CE has become a universal technique applied for identification and separation of many molecules from small to macromoleculars (Ban et al., 2001; Chen and Bartlett, 2012; Chen and Evangelista, 1998; Wang et al., 2006; Yu et al., 2004). Laser-induced fluorescence (LIF) detection has been used routinely in CE systems for detection of nucleotides and their applications due to its high sensitivity and selectivity compared to the UV detector (Li et al., 2014; Song et al., 2001). One challenge of CE consists in the selection of the separation buffer. This is particularly important for nanoparticles which exhibit a great tendency to aggregate into large superstructures. Such formations can occur during the CE analysis, resulting in an instable electrophoretic behavior. Another challenge, is the possible adsorption of analytes onto the inner surface of the fused silica capillary (Matczuk et al., 2015), accordingly we optimized the CE analytical conditions for MSN detection and quantification of siRNA loaded in and released from MSN.

2. Materials and methods

2.1. Chemicals

Two siRNA models targeted against PCSK9, sense sequence: GGAAGAUCAUAAUGGACAGdTdT, (Eurogenetec, Seraing, Belgium) were used. One without modification while the other was modified with Alexa 488, and referred to as Fl.siRNA (Sigma-Aldrich, St. Quentin Fallavier, France). Ferric chloride, ferric nitrate nonhydrate, chitosan high purity, MW 110,000–150,000, ammonium persulphate (APS), acrylamide, ribonuclease A, 3-(trimethoxysilyl)propyl methacrylate, ethidium bromide (Ethidium bromide solution 1%) and *N*,*N*,*N*′,*N*′-tetramethyl ethylene diamine (TEMED) were obtained from Sigma–Aldrich GmbH (Schnelldorf, Germany). Dulbecco's Modified Eagle Medium (DMEM) (ThermoFisher Scientific, Illkirch, France). Agarose (Invitrogen, Carlsbad, USA). Ammonia, sodium nitrate and sodium hydroxide were obtained from PROLABO Chemicals (Paris XI, France). Potassium hydroxide (LABOSI Chemicals, Paris, France), Ferrous chloride tetrahydrate, acetic acid, citric acid and Tris/acetate/EDTA buffer (TAE 1 ×, 40 mM Trisacetate, EDTA 1 mM, pH 7.6) were obtained from Acros Organics (Geel, Belgium). Nitric acid, acetone, methanol and disodium hydrogen phosphate dihydrate were obtained from CARLO ERBA Reagents S.A.S (Paris, France). All reagents were of analytical grades. Water was obtained from a Milli-Q system, Millipore, (Paris, France).

2.2. MSN preparation

SPION coated with covalently bound aminopropyl silanes (APTES) were prepared as reported by Hervé et al. (Hervé et al., 2008). MSN were formulated as described previously (David et al., 2013). Briefly, always equal volumes of siRNA solution and water on the one hand and silanised SPION, chitosan aqueous solution and water on the other hand were mixed together. The addition order was (1) water and (2) siRNA solution on the one hand and (1) water, (2) SPION and (3) chitosan on the other hand. Both volumes were vortexed separately and centrifuged with a micro centrifuge (6000 rpm, Model IR, Fischer Scientific, Illkirch, France), then mixed together using a micropipette. The quantity of each component was calculated upon mass ratio of iron (from SPION) to siRNA (MR = m(Fe)/m(siRNA)) and the charge ratio (CR) of positive chitosan charges to negative siRNA charges. MSN studied were prepared with siRNA concentration of 30 μg/mL, MR of 10 and CR of 44.

MSN purification was done *via* centrifugation (Sigma 3–30 K, Sigma laboratory centrifuges, Germany). After centrifugation at 6000*g* for 15 min, the supernatant was removed and replaced by the same volume of water (Milli-Q) then both supernatant and sediment were redispersed by vortexing for a few seconds.

2.3. MSN and siRNA analysis by capillary electrophoresis (CE)

2.3.1. Instrumentation

CE analysis was carried out using PACE MDQ (Beckman Coulter capillary electrophoresis system, USA) controlled by 32 Karat software (Version 8.0). This apparatus is equipped with a LIF detector with excitation by an air-cooled argon ion laser at a wavelength of 488 nm. The emission intensities were measured at a wavelength of 520 nm filtered by a band pass interference filter. Fused silica capillaries from Agilent technology, (USA) were used and they were 60 cm effective length and 75 μm ID. Capillaries were thermostated at 25 °C. The machine is also equipped with a diode array detector (DAD). UV detection took place at 220 nm for MSN and 272 nm for Fl.siRNA.

2.3.2. Capillaries preparation and coating

Uncoated capillaries were washed with NaOH 1 M for 5 min, followed by washing with water for 5 min before the first analysis. All washing were made at 20 p.s.i. For coated capillaries, the method described by Alejandro (Cifuentes et al., 1999) was used, etching was made by NaOH 1 M for 30 min, then leaching with HCl 0.1 M for 2 h at 20 p.s.i. After that, washing with water and methanol for 30 min and 10 min respectively was made at 20 p.s.i. Capillaries were then dried twice by air for 10 min at 20 p.s.i. Silylation solution was prepared by mixing 2 mL of 3-(trimethoxysilyl)propyl methacrylate, 2 mL methanol and 20 μL acetic acid. Capillary was exposed to the silylation solution for 30 min at 20 p.s.i and then allowed to stand within the solution for 16 h, then washed twice with methanol and water each for 10 min at 20 p.s.i. Coating solution was prepared by adding 7.5 μL ammonium

persulphate (APS)10% w/v and 7.5 µL *N,N,N′,N′*-tetramethyl ethylene diamine (TEMED) 10% v/v to a 3 mL of acrylamide solution 1% w/v. Capillaries were exposed to the coating solution for 30 min at 20 p.s.i and then allowed to stand within the solution for 6 h. Washing with water and buffer each for 1 min was made before each sample injection.

2.3.3. Analysis of nanocarriers before and after purification

Detection of MSN before and after purification was carried out using polyacrylamide coated capillaries. Citrate-phosphate buffer (pH 5, 5 mM) was used as the separation buffer. Samples were injected hydrodynamically for 5 s at 0.5 p.s.i by anodic injection at the short end of the capillary (− 25 kV, 10 cm). Fluorescence and UV detection were used.

2.3.4. Quantification of free Fl.siRNA in nanocarriers

For quantification of free Fl.siRNA in MSN before and after purification, citrate-phosphate buffer (pH 7, 2.5 mM) was used as the separation buffer. MSN were injected hydrodynamically for 5 s at 0.5 p.s.i by cathodic injection at the short end of the capillary (+ 25 kV, 10 cm), LIF detection. A linear calibration curve was obtained between 0.5 and 10 µg/mL as peak area $= 2{\cdot}10^6 * \text{Concentration} - 1 * 10^6$, with $R^2 = 0.9974$. At the lowest concentration, the relative standard deviation for peak area variability is about 3.6%, this concentration being then established as the limit of quantification (LOQ = 0.5 µg/mL $= 3.6 * 10^{-8}$ M). The precision of the method is demonstrated by RSD of peaks areas < 10% for each concentration level.

2.3.5. MSN colloidal stability assessment

The behavior of purified MSN (pMSN) at different pH ranging between 5 and 8.5 was studied. pMSN were always mixed with the buffer in the ratio of (1: 2, buffer: pMSN) by pipetting followed by vortexing for a few seconds. Citrate-phosphate buffer at a concentration of 25 mM was used for pH 5, 6 and 7.4, while Tris/acetate/EDTA (TAE) 1 × buffer was used for the pH 8.5. The samples were then characterized by capillary electrophoresis to study their aggregation profile as described in Section 2.3.3, and confirmed by size measurements.

2.3.6. In vitro siRNA release determination

The release kinetics of siRNA from pMSN suspended in citrate-phosphate buffer pH 7.4 (25 mM) and Dulbecco's Modified Eagle Medium (DMEM) pH 7.4 were studied. pMSN were always mixed with the buffer or the cell culture medium in the ratio of (1: 2, buffer or culture medium: pMSN) by pipetting followed by vortexing for a few seconds. The mixture was then divided into four aliquots and incubated at 37 °C for 1, 2, 4 and 24 h. After incubation, samples were centrifuged at 6000G for 15 min and the supernatant was analyzed for siRNA content using CE. Released siRNA was detected indirectly through complexation with chitosan by addition of a few microliters of concentrated chitosan solution (20 g/L) to the supernatant. Detection of Fl.siRNA chitosan complex was carried out using uncoated capillary. Sodium-phosphate buffer (pH 2, 10 mM) was used as separation buffer. Samples were injected hydrodynamically for 5 s at 0.5 p.s.i by anodic injection at the short end of the capillary (− 25 kV, 10 cm), LIF detection. A linear calibration curve for the Fl.siRNA chitosan complex was obtained at the concentration of Fl.siRNA between 0.5 and 30 µg/mL as Peak area $= 443311 * \text{Concentration} + 34525$, $R^2 = 0.9991$. At the lowest concentration, the relative standard deviation for peak area variability is 6%, this concentration being then established as the limit of quantification (LOQ = 0.5 µg/mL $= 3.6 * 10^{-8}$ M). The precision of the method is demonstrated by RSD of peaks areas < 10% for each concentration level. The amount of the Fl.siRNA released at each condition was calculated as a percentage referring to the initial quantity used for formulation (corresponding to 30 µg/mL).

2.3.7. Study of siRNA degradation by ribonuclease enzymes

Purified MSN were studied for their ability to protect siRNA from degradation by ribonuclease A enzymes. The enzyme (1.2 µg/mL) was added to pMSN in the ratio of (1: 2, enzyme: pMSN) and mixed by pipetting followed by vortexing for a few seconds. The mixture was then divided into four aliquots and incubated at 37 °C for 1, 2, 4 and 24 h. Samples were analyzed by CE-LIF as described in Section 2.3.3 and confirmed by AGE.

The percentage of protection efficiency was calculated as follow:

$$\text{Protection efficiency} = \frac{\textbf{\textit{Average peak area of pMSN at time }}(\boldsymbol{t})}{\textbf{\textit{Average peak area of pMSN before addition of the enzyme}}} \times 100$$

2.4. MSN size and surface charge determination

Mean hydrodynamic diameter (D_H) of the samples was measured using a High Performance Particle Sizer (HPPS) (Malvern Instruments, Malvern, UK). Before measurement, the nanocarriers were diluted in $NaNO_3$ 0.01 M at a ratio of 1:25. The pH of the media was 6.1. The D_H measurements of the nanocarriers were done in triplicate with automatic setting of the measurement parameters. The position of the laser was fixed at 2.0 mm for a better comparison of the measurements.

The surface charge of the nanocarriers, in term of their zeta potential, was measured using a Malvern NanoZ zetameter (Malvern Instruments, Malvern, UK) using the same samples as for the D_H measurements. Each measurement was done in triplicate.

2.5. Analysis of siRNA complexation by agarose gel electrophoresis (AGE)

10 µL of sample and 5 µL of water or 5 µL of KOH (0.1 M) were mixed before adding 1.5 µL of Agarose gel loading dye 6 ×. (Fisher Bioreagents®, Illkirch, France). KOH was added to liberate siRNA from the complexes to verify their integrity after formulation.

The prepared samples were then deposited on 1% agarose gel containing 0.01% ethidium bromide, prepared with pure agarose and a Tris/acetate/EDTA 1 × buffer, to migrate for about 15 min at 100 V. Images were taken using Fusion Solo. S6® imager (WL. Vilber Lourmat, Marne la Vallée, France) and analyzed with the Evolution Capt Software. Before analysis of the samples used in the study of siRNA protection against RNAse A, RNAse activity was inhibited by heating the sample for 30 min at 70 °C.

2.6. Quantification of MSN components by UV–visible spectrophotometry

UV–visible spectra of MSN before and after purification and the different MSN components were acquired with a GENESYS® 10s, UV–visible spectrophotometer (Thermo Scientific, Illkirch, France). Treatment of spectra were performed with LABSPEC 4.04 software. Each experimental spectrum was fitted using the classical least-squares method to a sum of the two reference spectra of siRNA and SPION-chitosan. In parallel, a linear calibration curve was obtained between 0.0039 and 0.011 µg/mL as Absorbance $= 0.0024 * \text{Concentration} + 0.0027$, with $R^2 = 0.999$ for Fl.siRNA. For SPION, linear calibration curve was obtained from SPION chitosan mixture between 0.015 and 0.03 mg/mL as Absorbance $= 44.4 * \text{Concentration} + 0.211$, with $R^2 = 0.999$.

3. Results and discussion

3.1. Capillary electrophoresis (CE) – an interesting analytical tool for MSN characterization

Capillary electrophoresis (CE) is a separation method based on the different electrophoretic mobilities of charged molecules under the effect of an electric field. Typically, separation takes place in a capillary of small diameter (usually 50–100 µm), requiring small amount of

samples for the analysis. Previously, we have used this method in our research on the distribution of doxorubicin drug-loaded magnetic nanovectors in cancer cells (Gautier et al., 2015). CE is a method of high efficiency and the use of laser-induced fluorescence as detection method provides high sensitivity. However, the main problem to be overcome in CE is usually the potential interactions of the analyte with the surface of the capillary. In order to reduce these interactions, various modifications of the capillary inner wall surface are available but need to be optimized (Cifuentes et al., 1999). In the present work, we have used CE to characterize nanoparticles made of several constituents associated by electrostatic interactions. One of the major component is chitosan biopolymer which constitutes the external coating layer of the nanoparticles. At pH range of 5 to 6 used to formulate MSN, chitosan is positively charged and contributes in electrostatic interactions of the MSN with the negative surface of the capillary. In order to reduce these interactions, we chemically modified the capillary wall with neutral polyacrylamide molecules.

Moreover, CE analysis of nanoparticles is more challenging and quite different from study of molecules in solution. Indeed, CE requires to use background buffers to provide separation medium. If the ionic strength of the buffer is too high, ionic cloud surrounding nanoparticles can be compressed and the stability of the system can be affected (López-Lorente et al., 2011). We investigated various separation buffer systems in terms of their composition and pH. The results showed that the optimal MSN analysis conditions were obtained with citrate-phosphate buffer at a low concentration (pH 5, 2.5 mM) whereas the same buffer at a concentration of 5 mM was optimal for MSN formulated with Fl.siRNA. Two methods of detection were used: diode array detector (DAD) is implemented in every commercial CE system for its simplicity. However, its sensitivity is limited. On the other hand, laser induced fluorescence (LIF) detection is known to have nearly 1000 fold higher sensitivity and better selectivity compared to UV–vis detection. UV detection of MSN was based on the light scattering-related absorbance of SPION core of the nanovectors at 220 nm, while LIF-based detection was possible only for MSN loaded with the Fl.siRNA. After analysis of Fl.MSN, typical spectra of SPION (data not shown) was observed for a peak at 2.12 ± 0.14 min while a signal of fluorescence was detected at a similar migration time with CE-LIF detection (Fig. 1A and B). The agreement in the migration time of these two peaks by UV and fluorescence demonstrates that these signals can be assigned to the nanocarriers.

These results were in agreement with the agarose gel electrophoresis (AGE) data (Fig.1D). During the AGE analysis, ethidium bromide incorporated in agarose gel intercalates free siRNA molecules and produces a fluorescence band upon UV excitation. Complexed siRNA molecules are less accessible to ethidium bromide and do not migrate in the agarose gel. For the MSN, a fluorescence band observed in the gel was very weak compared to siRNA solution. This indicates that the major part of siRNA in MSN was bound to the nanoparticles. An increase of the pH, by addition of KOH, suppressed the chitosan positive charges, destabilized MSN and liberated siRNA. As a result, an intense fluorescence band, comparable to that of the control siRNA, was observed, indicating high siRNA payload in MSN.

3.2. Physical and chemical characteristics of MSN

Pharmaceutical quality and safety requirements for MSN as potential nanomedicine treatment involves control of several parameters, like the medium purity in terms of possible presence of residual free components, nanoforms structure and composition and their colloidal and chemical stability (Itoh et al., 2015).

CE results for MSN before and after purification by centrifugation showed that a first centrifugation at 6000*g* yields the required purity for MSN remaining in the supernatant (thereafter called pMSN) with few aggregates being in the sediment (Fig. 1A and B). This was even more apparent when LIF detector was used (Fig.1B). These results are in

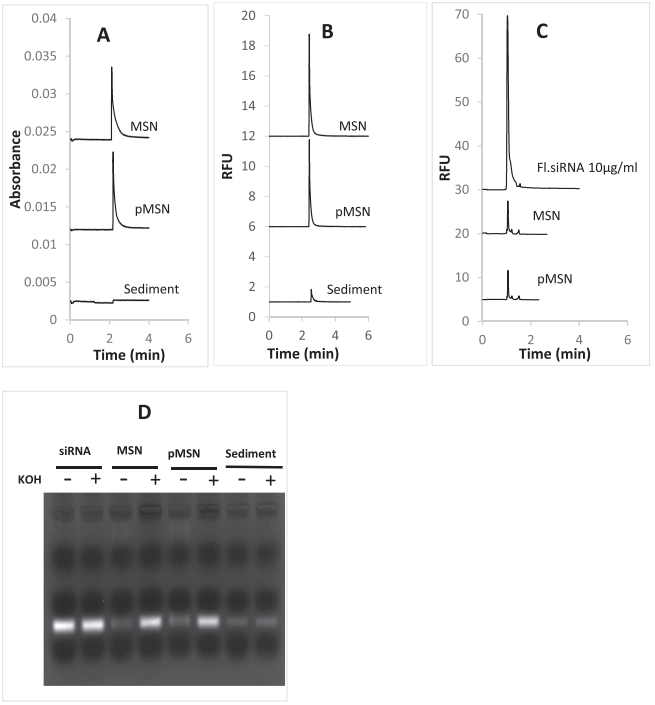

Fig. 1. Purification of MSN: Electropherograms showing: (**A**) UV detection of Fl.MSN at 220 nm. (**B**) LIF detection of Fl.MSN. (**C**) LIF detection of free Fl.siRNA. CE conditions: Polyacrylamide coated capillary 75 µm ID × 60 cm, hydrodynamic injection for 5 s. at 0.5 p.s.i, 25 °C. (**A** and **B**) Citrate phosphate buffer pH 5 (5 mM), applied voltage − 25 kV, anodic injection. (**C**) Citrate phosphate buffer pH 7 (2.5 mM), applied voltage + 25 kV, cathodic injection. (**D**) Agarose gel electrophoresis of MSN before and after purification. The first condition of the sample (−) is without KOH indicating free siRNA in this condition, the second condition of the sample (+) is with KOH indicating the total amount of siRNA in the sample.

agreement with the hypothesis that the centrifugation at low speed removed larger MSN and/or SPION aggregates while less dense individual small MSN remained in the supernatant. A second centrifugation was made at higher strength (20,000*g*), to precipitate individual MSN in the second sediment while allowing residual free molecular components (if found) to remain in the second supernatant. However, because of the high colloidal stability of MSN, such separation was not achieved: MSN were still present in the second supernatant and only few MSN in the second sediment (data not shown). These results confirm that the protocol of MSN formulation was already well optimized. After purification, the values of D_H, measured in aqueous medium (pH 6.1 and ionic strength 0.01 mol/L), decreased from *ca.*100 nm to *ca.* 80 nm (Table 1). The polydispersity index (PDI), indicating if the sample has a monomodal size distribution or if there are several populations in the sample, diminished slightly after purification from 0.33 to 0.29. This is in agreement with the elimination of bigger aggregates or free SPION. The zeta potential (*i.e.* the surface charge of MSN represented by the ions forming an electrical double layer around MSN) decreased from *ca.* + 20 mV to *ca.* + 15 mV, probably due to elimination of free SPION carrying a lot of positive charges due to their aminosilane-modified surface. This hypothesis was supported by the brown color of the sediment and confirmed by atomic absorption

Table 1
Comparison between the nanovectors before (**MSN**) and after purification (**pMSN**).

Formulation	MSN	pMSN
D_H (nm)	93.71 ± 20.56	79.16 ± 6.82
PDI	0.33 ± 0.05	0.29 ± 0.05
Zeta potential (mV)	20.49 ± 13.46	14.92 ± 12.42
Mass ratio (m_{Fe}/m_{siRNA})	9.4	6.5

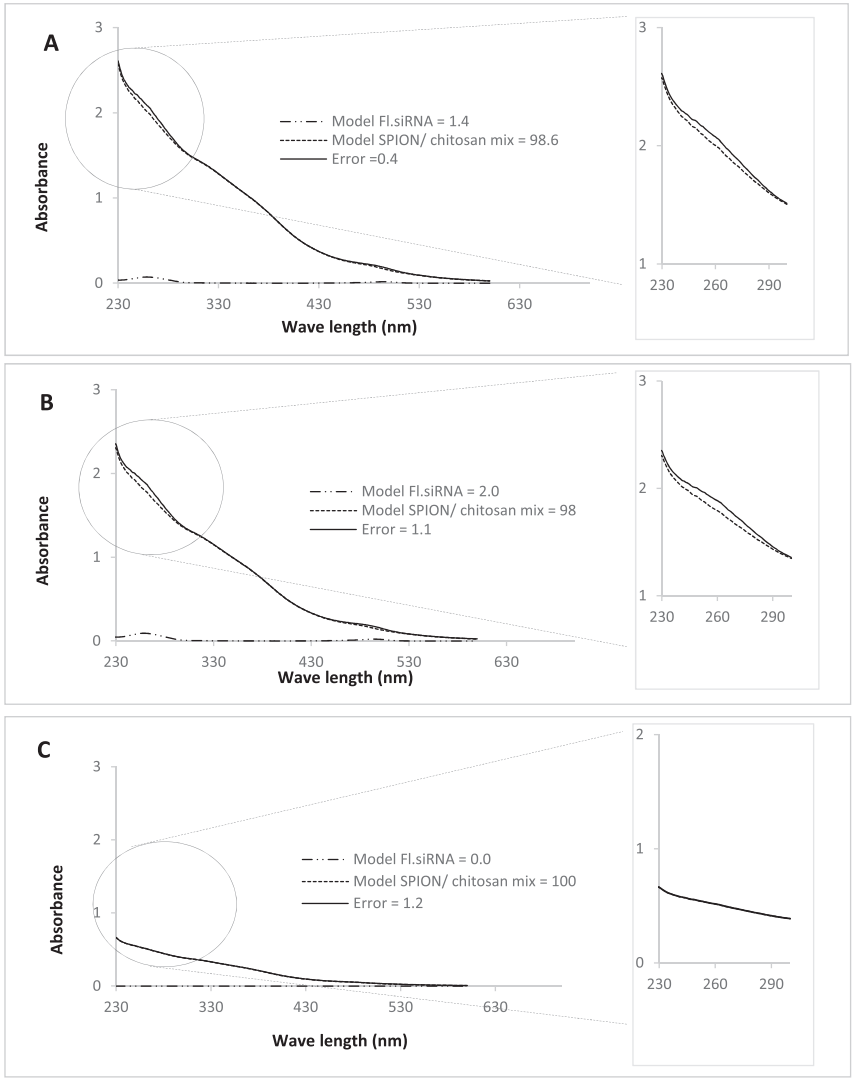

Fig. 2. Quantification of MSN components, representative curve fitting of (**A**) MSN (**B**) pMSN and (**C**) the sediment. The contribution of each component is represented.

spectroscopy (data not shown).

CE technique has also been used to check the presence or absence of free siRNA in pMSN. In that case, MSN were loaded with Fl.siRNA for CE-LIF analysis. The optimum analysis medium was the citrate-phosphate buffer at pH 7 (2.5 mM). Fl.siRNA migration time was 1.05 ± 0.02 min (Fig. 1C). As described in the experimental section, the analytical methodology validation included calibration curve from which the limit of quantification was deduced. Quantification of Fl.siRNA from the electropherograms of MSN and pMSN showed that they contain 1.69 and 1.41 µg/mL of free Fl.siRNA, respectively. In comparison to the theoretical concentration of 30 µg/mL, these results allow to demonstrate that free siRNA content is about 5%. The free Fl.siRNA content determined with CE is in agreement with the intensity of the fluorescence bands observed in AGE (Fig. 1D).

The siRNA loading within pMSN was estimated from their UV–vis spectra, by fitting them with separately recorded spectra of Fl.siRNA and of SPION & chitosan mixture (Fig.2). The fitting errors were typically below 2% of the total spectral area. The obtained results indicated that no Fl.siRNA was found in the sediment of the purification step. Calibration curve obtained from the UV–vis absorption of Fl. siRNA in aqueous solution enabled us to establish that: the concentration of siRNA in MSN before purification (29.3 ± 1.44 µg/mL) was logically similar to that used for formulation (30 µg/mL) and corresponding to the mass of 5.87 ± 0.29 µg. Similar calculations for SPION gave a mass of 55 ± 2.5 µg of iron instead of 60 µg. Thus the mass ratio (MR) calculated as iron content of SPION to siRNA corresponds to 9.4. For pMSN, the mass of Fl.siRNA and iron were found 6.4 ± 0.3 µg and 41.8 ± 3.89 µg respectively (MR: 6.5). The Fl.siRNA loading rate was the same before and after the MSN purification. However, the MR decreased from 9.4 to 6.5 due to the loss of some SPION as aggregates in the sediment after purification. This is in agreement with previous results indicating that a MR between 5 and 7.5 is needed for a complete siRNA complexation with SPION (David et al., 2013). However, smaller MSN sizes were obtained when a MR of 10 was used for the MSN formulation.

In summary, these results show that the centrifugation applied as a method of purification lead to a higher siRNA proportion in pMSN compared to non-purified MSN and especially no valuable raw material loss. The purification could be very useful for a future *in vivo* application as the aim is to carry a sufficient amount of siRNA in pMSN. Thereafter, for further MSN development we will study only the purified MSN (pMSN).

3.3. Influence of pH on colloidal stability

CE was also used, to analyze the colloidal stability of pMSN. Throughout the process of manufacture and storage, pMSN should be stable over a wide pH range to ensure the robustness of the method on the one hand and the safe siRNA delivery on the other hand. CE data (Fig. 3A) indicated that pMSN were resistant against aggregation at

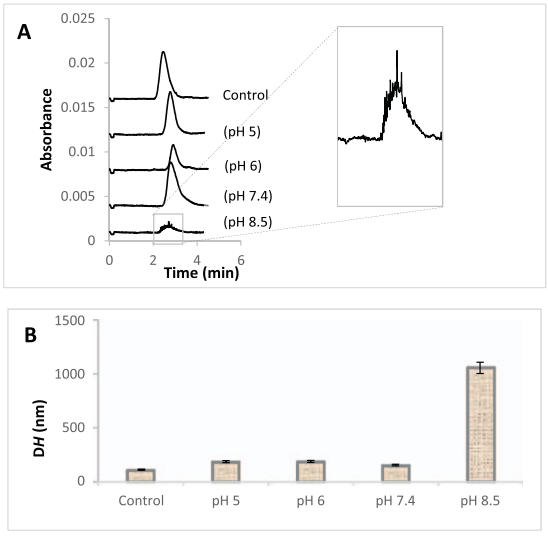

Fig. 3. Colloidal stability of purified MSN at different pH. (**A**) Electropherograms showing behavior of the purified MSN at different pH. CE conditions: Polyacrylamide coated capillary 75 μm ID × 60 cm, Citrate phosphate buffer pH 5 (2.5 mM), applied voltage − 25 kV, anodic hydrodynamic injection for 5 s. at 0.5 p.s.i 25 °C,UV detection at 220 nm. (**B**) Hydrodynamic diameter of purified MSN at different pH. Control = pMSN.

pH 5, 6 and 7.4 since no modifications in the peaks shape and migration time were noticed. At pH 8.5, the nanovectors were immediately prone to aggregation as indicated by presence of spikes. In the past, CE was used to analyze iron oxide nanoparticles and it has been shown that, if instability occurs, groups of spikes are visible on the electropherogram instead of the Gaussian-shaped peaks (Vanifatova et al., 2005). The CE results were concomitant with the hydrodynamic diameter values of pMSN (Fig. 3B): pMSN size was similar at pH 5, 6 and 7.4 while it increased at pH 8.5. The instability of pMSN at pH 8.5 is probably due to the loss of balance of attractive-repulsive forces between nanoparticles. Indeed, the pKa of chitosan is 6.5 (Buchman et al., 2013; M. et al., 2012) indicating that it should be less charged at pH above 6.5. The good colloidal stability of MSN at pH up to 7.4 was encouraging for their biological evaluation.

3.4. Release of siRNA at pH 7.4 and its protection against ribonuclease enzymes

The *in vitro* release profiles of Fl.siRNA from pMSN were established for 24 h at pH 7.4, in both citrate-phosphate buffer and in cell culture medium DMEM. After incubation, we noticed that, pMSN started to separate into two phases with a clear supernatant. We expected a concomitant release of chitosan followed by complexation with siRNA. This hypothesis was confirmed by analysis of siRNA-chitosan complex solution and observation of reproducible peaks for this complex using uncoated capillaries with sodium-phosphate buffer pH 2, 10 mM as separation buffer, by CE-LIF detection. Thus, we decided to add concentrated chitosan solution to the each supernatant obtained from release experiments to ensure detection of the whole siRNA quantity.

siRNA release was found higher in the DMEM cell culture medium (10%) than in the citrate-phosphate buffer (3%) after 1 h. With time, the quantity of released siRNA decreased and may be undetectable in citrate phosphate buffer (Fig. 4A). The siRNA release in the first hour can be explained by diffusion of siRNA bound near the particles surfaces due to dilution. This behavior is similar to that described by A.G. Raja et al. using crosslinked chitosan-siRNA nanoparticles (Abdul Ghafoor Raja et al., 2015). However, in our case, the siRNA release is decreased at later stage which could be explained by a supposable re-inclusion of released siRNA to the (aggregated) MSN.

Efficient gene delivery system is also dependent upon the ability of the carrier to protect its payload from nuclease degradation. For

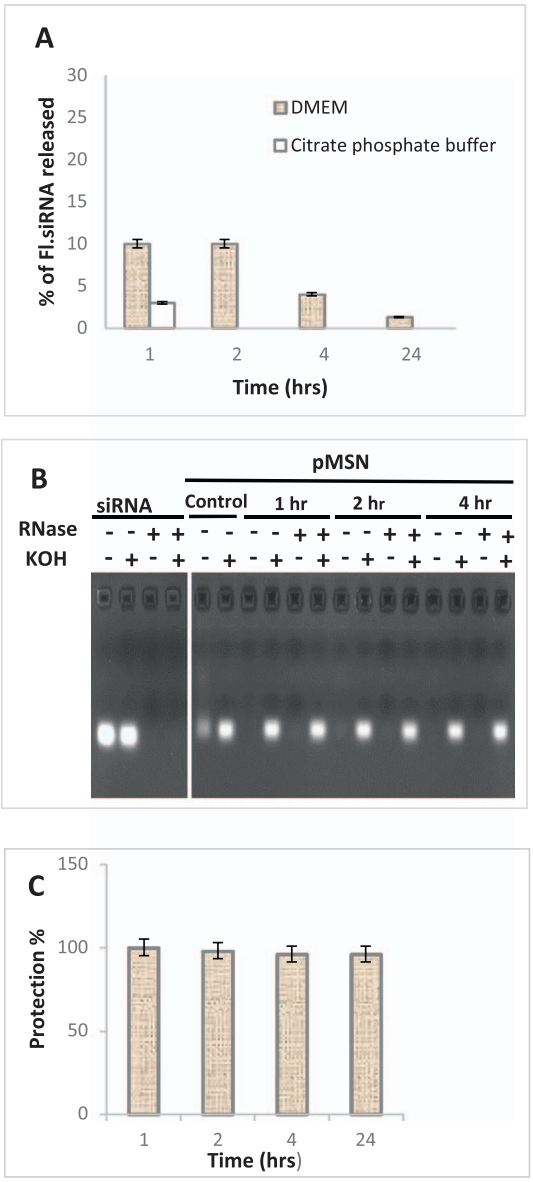

Fig. 4. siRNA release and protection against ribonuclease enzymes (**A**) Histograms showing the *in vitro* release profile of Fl.siRNA from the purified MSN at pH 7.4. The % amount of Fl.siRNA released was determined using CE-LIF detection. CE conditions: uncoated capillary 75 μm ID × 60 cm, 25 °C, hydrodynamic injection for 5 s. at 0.5 p.s.i. Na-phosphate buffer pH 2 (10 mM)), applied voltage − 25 kV, anodic injection. (**B**) Agarose gel electrophoresis of purified MSN in presence (+) or absence (−) of ribonuclease A (RNAse) and KOH. Control = pMSN without addition of RNAse. (**C**) Histograms showing protection of Fl.siRNA against ribonuclease A by MSN using capillary electrophoresis. CE conditions: Polyacrylamide coated capillary 75 μm ID × 60 cm, 25 °C, hydrodynamic injection for 5 s. at 0.5 p.s.i. Citrate phosphate buffer pH 5 (5 mM), applied voltage − 25 kV, anodic injection, LIF detection.

maximal activity in the cells, siRNA must be protected from digestion by nucleases as free siRNA are rapidly degraded (< 30 min) by RNAse (Haupenthal et al., 2006). Fig. 4B shows the siRNA integrity study by AGE indicating a highly efficient siRNA protection toward degradation by ribonucleases. A weak fluorescent band was observed with the initial pMSN as already seen above. The control free siRNA were rapidly degraded by RNAse, as there was no fluorescence band observed after 30 min of incubation. However, for purified MSN both in presence and in absence of ribonuclease, there was no fluorescence in absence of KOH. In contrast, after addition of KOH to the samples, there was an intense band of fluorescence, similar to that of the control sample (siRNA alone). In addition, CE data for pMSN (Fig. 4C) show that the

siRNA enzymatic degradation was hindered up to 24 h, with protection efficiency of 96%. Interestingly, the purification step did not interfere with this protection. In the literature, depending on the type of nanocarriers, one finds that the duration of the siRNA protection against serum or RNAse A *in vitro* (at 37 °C) varied from few minutes to 48 h (Resnier et al., 2013). The result obtained in our study with pMSN is encouraging. Further experiments with pMSN in serum and *in vivo* will be made in the close future.

4. Conclusion

Based on the findings of the present study, we conclude that stable purified magnetic siRNA nanovectors (MSN) possess properties potentially suitable for their systemic administration. In addition, the study includes the optimization of analytical conditions for MSN characterization by CE with DAD detector and CE-LIF. Purification by centrifugation allowed to remove free SPION and therefore to increase the siRNA/SPION ratio in MSN. Purified MSN had smaller sizes, lower PDI and lower zeta potential. At pH 7.4, < 10% of loaded siRNA were released in 24 h, while no MSN aggregation was observed. The nanovectors efficiently protected siRNA against degradation by RNAse A. In summary, MSN demonstrated promising properties for their further evaluation *in vitro* and/or *in vivo* as well as for a perspective of their application in cancer theranosis. However, pMSN stability and efficacy may be improved by addition of polymers and/or targeting ligands.

Conflict of interest

The authors confirm that this article content has no conflicts of interest.

Acknowledgements

The authors would like to thank the “Institut National du Cancer (INCa)”, the “Fondation ARC” and the “Ligue nationale contre le cancer (LNCC)” (ARC_INCa_LNCC_7636) for the financial support and Didier Bedin (EA6295, “Nanomédicaments et Nanosondes”, University François Rabelais of Tours) for technical support.

References

Abdul Ghafoor Raja, M., Katas, H., Jing Wen, T., 2015. Stability, intracellular delivery, and release of siRNA from chitosan nanoparticles using different cross-linkers. PLoS One 10. http://dx.doi.org/10.1371/journal.pone.0128963.

Ban, E., Choi, O.-K., Ryu, J.-C., Yoo, Y.S., 2001. Capillary electrophoresis of high-molecular chitosan: the natural carbohydrate biopolymer. Electrophoresis 22, 2217–2221. http://dx.doi.org/10.1002/1522-2683(20017)22:11<2217::AID-ELPS2217>3.0.CO;2-R.

Bennett, K.M., Jo, J., Cabral, H., Bakalova, R., Aoki, I., 2014. MR imaging techniques for nano-pathophysiology and theranostics. Adv. Drug Deliv. Rev. 74, 75–94. http://dx.doi.org/10.1016/j.addr.2014.04.007.

Buchman, Y.K., Lellouche, E., Zigdon, S., Bechor, M., Michaeli, S., Lellouche, J.-P., 2013. Silica nanoparticles and polyethyleneimine (PEI)-mediated functionalization: a new method of PEI covalent attachment for siRNA delivery applications. Bioconjug. Chem. 24, 2076–2087. http://dx.doi.org/10.1021/bc4004316.

Buschmann, M.D., Merzouki, A., Lavertu, M., Thibault, M., Jean, M., Darras, V., 2013. Chitosans for delivery of nucleic acids. Adv. Drug Deliv. Rev. 65, 1234–1270. http://dx.doi.org/10.1016/j.addr.2013.07.005.

Chen, B., Bartlett, M.G., 2012. Determination of therapeutic oligonucleotides using capillary gel electrophoresis. Biomed. Chromatogr. 26, 409–418. http://dx.doi.org/10.1002/bmc.1696.

Chen, F.T., Evangelista, R.A., 1998. Profiling glycoprotein n-linked oligosaccharide by capillary electrophoresis. Electrophoresis 19, 2639–2644. http://dx.doi.org/10.1002/elps.1150191512.

Cifuentes, A., Canalejas, P., Diez-Masa, J.C., 1999. Preparation of Linear Polyacrylamide-Coated Capillaries - Study of the Polymerization Process and Its Effect on Capillary Electrophoresis Performance. http://dx.doi.org/10.1016/S0021-9673(98)00923-6.

David, S., Marchais, H., Hervé-Aubert, K., Bedin, D., Garin, A.-S., Hoinard, C., Chourpa, I., 2013. Use of experimental design methodology for the development of new magnetic siRNA nanovectors (MSN). Int. J. Pharm. 454, 660–667. http://dx.doi.org/10.1016/j.ijpharm.2013.05.051.

David, S., Marchais, H., Bedin, D., Chourpa, I., 2014. Modelling the response surface to predict the hydrodynamic diameters of theranostic magnetic siRNA nanovectors. Int. J. Pharm. 478, 409–415. http://dx.doi.org/10.1016/j.ijpharm.2014.11.061.

Devarasu, T., Saad, R., Ouadi, A., Frisch, B., Robinet, E., Laquerrière, P., Voegel, J.-C., Baumert, T., Ogier, J., Meyer, F., 2013. Potent calcium phosphate nanoparticle surface coating for in vitro and in vivo siRNA delivery: a step toward multifunctional nanovectors. J. Mater. Chem. B 1, 4692–4700. http://dx.doi.org/10.1039/C3TB20557F.

Estelrich, J., Sánchez-Martín, M.J., Busquets, M.A., 2015. Nanoparticles in magnetic resonance imaging: from simple to dual contrast agents. Int. J. Nanomedicine 10, 1727–1741. http://dx.doi.org/10.2147/IJN.S76501.

Gautier, J., Munnier, E., Soucé, M., Chourpa, I., Douziech Eyrolles, L., 2015. Analysis of doxorubicin distribution in MCF-7 cells treated with drug-loaded nanoparticles by combination of two fluorescence-based techniques, confocal spectral imaging and capillary electrophoresis. Anal. Bioanal. Chem. 407, 3425–3435. http://dx.doi.org/10.1007/s00216-015-8566-9.

Haupenthal, J., Baehr, C., Kiermayer, S., Zeuzem, S., Piiper, A., 2006. Inhibition of RNAse A family enzymes prevents degradation and loss of silencing activity of siRNAs in serum. Biochem. Pharmacol. 71, 702–710. http://dx.doi.org/10.1016/j.bcp.2005.11.015.

Haussecker, D., 2014. Current issues of RNAi therapeutics delivery and development. J. Control. Release 195, 49–54. http://dx.doi.org/10.1016/j.conrel.2014.07.056.

Hervé, K., Douziech-Eyrolles, L., Munnier, E., Cohen-Jonathan, S., Soucé, M., Marchais, H., Limelette, P., Warmont, F., Saboungi, M.L., Dubois, P., Chourpa, I., 2008. The development of stable aqueous suspensions of PEGylated SPIONs for biomedical applications. Nanotechnology 19, 465608. http://dx.doi.org/10.1088/0957-4484/19/46/465608.

Itoh, N., Santa, T., Kato, M., 2015. Rapid and mild purification method for nanoparticles from a dispersed solution using a monolithic silica disk. J. Chromatogr. A 1404, 141–145. http://dx.doi.org/10.1016/j.chroma.2015.05.047.

Juliano, R., Alam, M.R., Dixit, V., Kang, H., 2008. Mechanisms and strategies for effective delivery of antisense and siRNA oligonucleotides. Nucleic Acids Res. 36, 4158–4171. http://dx.doi.org/10.1093/nar/gkn342.

Li, Z., Liu, C., Yamaguchi, Y., Ni, Y., You, Q., Dou, X., 2014. Capillary electrophoresis of a wide range of DNA fragments in a mixed solution of hydroxyethyl cellulose. Anal. Methods 6, 2473–2477. http://dx.doi.org/10.1039/C3AY41965G.

Limayem, I., Charcosset, C., Fessi, H., 2004. Purification of nanoparticle suspensions by a concentration/diafiltration process. Sep. Purif. Technol. 38, 1–9. http://dx.doi.org/10.1016/j.seppur.2003.10.002.

López-Lorente, A.I., Simonet, B.M., Valcárcel, M., 2011. Electrophoretic methods for the analysis of nanoparticles. TrAC Trends Anal. Chem. 30, 58–71. http://dx.doi.org/10.1016/j.trac.2010.10.006.

Malmo, J., Sørgård, H., Vårum, K.M., Strand, S.P., 2012. siRNA delivery with chitosan nanoparticles: Molecular properties favoring efficient gene silencing. J. Control. Release 158, 261–268. http://dx.doi.org/10.1016/j.jconrel.2011.11.012.

Matczuk, M., Aleksenko, S.S., Matysik, F.-M., Jarosz, M., Timerbaev, A.R., 2015. Comparison of detection techniques for capillary electrophoresis analysis of gold nanoparticles. Electrophoresis 36, 1158–1163. http://dx.doi.org/10.1002/elps.201400597.

Meister, G., Tuschl, T., 2004. Mechanisms of gene silencing by double-stranded RNA. Nature 431, 343–349.

Pedro, L., Soares, S.S., Ferreira, G.N.M., 2008. Purification of bionanoparticles. Chem. Eng. Technol. 31, 815–825. http://dx.doi.org/10.1002/ceat.200800176.

Resnier, P., Montier, T., Mathieu, V., Benoit, J.-P., Passirani, C., 2013. A review of the current status of siRNA nanomedicines in the treatment of cancer. Biomaterials 34, 6429–6443. http://dx.doi.org/10.1016/j.biomaterials.2013.04.060.

Song, L., Liang, D., Chen, Z., Fang, D., Chu, B., 2001. DNA sequencing by capillary electrophoresis using mixtures of polyacrylamide and poly(*N*,*N*-dimethylacrylamide). J. Chromatogr. A 915, 231–239. http://dx.doi.org/10.1016/S0021-9673(01)00593-3.

Vanifatova, N.G., Spivakov, B.Y., Mattusch, J., Franck, U., Wennrich, R., 2005. Investigation of iron oxide nanoparticles by capillary zone electrophoresis. Talanta 66, 605–610. http://dx.doi.org/10.1016/j.talanta.2004.12.016.

Wang, Q., Xu, X., Dai, L., 2006. A new quasi-interpenetrating network formed by poly(N-acryloyl-tris-(hydroxymethyl))aminomethane and polyvinylpyrrolidone: separation matrix for double-stranded DNA and single-stranded DNA fragments by capillary electrophoresis with UV detection. Electrophoresis 27, 1749–1757. http://dx.doi.org/10.1002/elps.200500597.

Xu, C., Wang, J., 2015. Delivery systems for siRNA drug development in cancer therapy. Asian J. Pharm. Sci. 10, 1–12. http://dx.doi.org/10.1016/j.ajps.2014.08.011.

Yu, R.Z., Geary, R.S., Monteith, D.K., Matson, J., Truong, L., Fitchett, J., Levin, A.A., 2004. Tissue disposition of 2′-O-(2-methoxy) ethyl modified antisense oligonucleotides in monkeys. J. Pharm. Sci. 93, 48–59. http://dx.doi.org/10.1002/jps.10473.